Geophysical Research Letters

RESEARCH LETTER
10.1029/2018GL079983

Key Points:
- Hydroacoustic arrivals at Wake Island can be linked to the 2014 eruption at Ahyi volcano
- Signal frequency and magnitude evolved over the course of the episode, indicating changes in source parameters
- Acoustic energy released during the eruption contributed significantly to the ocean soundscape

Supporting Information:
- Supporting Information S1

Correspondence to:
D. Metz,
dmetz@jamstec.go.jp

Citation:
Metz, D., & Grevemeyer, I. (2018). Hydroacoustic measurements of the 2014 eruption at Ahyi volcano, 20.4°N Mariana Arc. *Geophysical Research Letters*, *45*, 11,050–11,058. https://doi.org/10.1029/2018GL079983

Received 9 AUG 2018
Accepted 27 SEP 2018
Accepted article online 8 OCT 2018
Published online 20 OCT 2018

Hydroacoustic Measurements of the 2014 Eruption at Ahyi Volcano, 20.4°N Mariana Arc

D. Metz[1] and I. Grevemeyer[2]

[1]Research and Development Center for Earthquake and Tsunami, Japan Agency for Marine-Earth Science and Technology (JAMSTEC), Yokohama, Japan, [2]GEOMAR Helmholtz Centre for Ocean Research Kiel, Kiel, Germany

Abstract Ahyi is a fully submerged arc volcano in the Northern Mariana Islands, northwestern Pacific Ocean. In April and May 2014, the volcano erupted over a period of 15 days. Results from direction-of-arrival calculations show that underwater sound phases associated with the episode were recorded as far as Wake Island, where a hydrophone triplet array is operated as part of the International Monitoring System. After a 3.5-hr-long sequence of hydroacoustic precursory events, explosive volcanic activity occurred in two distinct, several-days-long bursts, accompanied by a notable decrease in low-frequency arrivals that may indicate a shift in signal source parameters. Acoustic resolution of the hydrophone data supersedes broadband networks by almost 1 order of magnitude, successfully identifying seismic events at Ahyi as low as 2.5 m_b. Total radiated acoustic energy of the eruption is estimated at 9.7 10^{13} J, which suggests that submarine volcanic activity contributed significantly to the ocean soundscape.

Plain Language Summary Little is known about active volcanism in the global ocean due to the inherent inaccessibility of the marine environment for conventional monitoring techniques. Here we resort to long-range hydroacoustic measurements to study the 2014 eruption of Ahyi, an active submarine volcano located in the Mariana Arc, northwestern Pacific Ocean. We show that underwater sound phases associated with the 2014 eruption of the volcano were recorded by hydrophones of the International Monitoring System, a global sensor network maintained by the Comprehensive Nuclear-Test-Ban Treaty Organization. Hydroacoustic data suggest that several precursory events preceded the 2-week-long, main eruptive episode, potentially indicating the collapse of the magma chamber and the subsequent intrusion of material into the volcanic conduit. We observe a relative decrease in lower-frequency arrivals toward the end of the eruption, which we attribute to changes in signal source parameters inside the edifice. The resolution of the International Monitoring System hydrophones supersedes broadband data recorded at land-based seismometers in the region, detecting seismic activity at Ahyi as low as 2.5 m_b. In a final step, we estimate the substantial acoustic energy release of the eruption and conclude that natural sources of underwater sound should be taken into account when studying the ocean soundscape.

1. Introduction

Ahyi is a submarine volcano located at 20.42°N, 145.03°E in the northern Mariana Arc, northwestern Pacific Ocean (Figure 1a). The edifice consists of a 12-km-wide, hydrothermally active stratovolcanic cone that rises from approximately 2,000 to 70 m below sea level at a location 20 km southeast of Farallon de Pajaros (formerly Uracas), the northernmost island in the Northern Marianas Islands chain (Bloomer et al., 1989; Resing et al., 2009, Figure 1b). Reports of eruptive activity at Ahyi include discolored surface waters in 1979 (Global Volcanism Program, 1979) and observations of seismic tertiary waves ("T phases") throughout the South Pacific region in 2001 (Global Volcanism Program, 2001). Volcanic episodes in the area date back until at least 1967, when hydrophones of the Sound Surveillance System recorded a high incidence of underwater explosion sounds from a location 10 km southeast of Farallon de Pajaros (Norris & Johnson, 1969), indicating a possible source near Makhahnas Seamount. Further activity has been intermittently observed near Supply Reef, a shallow submarine volcano 30 km northwest of Maug Island, in 1969 and on at least three occasions in the 1980s (Global Volcanism Program, 2001).

In April and May 2014, Ahyi erupted over the course of approximately 2 weeks. Onsite observations included explosions heard by scuba divers and aboard ships in the area, as well as conglomerates of ejected material

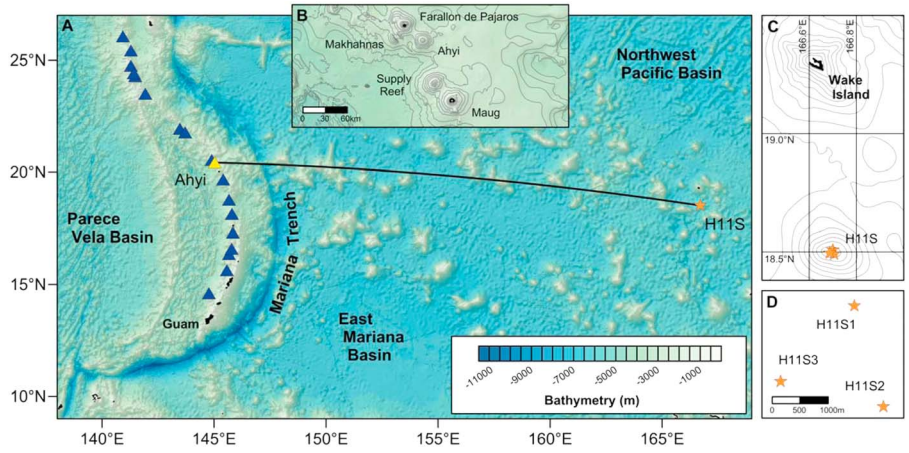

Figure 1. Overview map. (a) Locations of Ahyi volcano (yellow triangle) and the H11S hydrophone array (orange star) in the northwestern Pacific Ocean. The blue triangles represent volcanic edifices with observed or inferred eruptive activity over the last 2,000 years according to the Smithsonian Global Volcanism Database (Global Volcanism Program, 2013). The source-receiver distance between the volcano and H11S (black line) is 2,283 km at a geodesic back azimuth of 278.9°. (b) Detailed view of the seafloor topography south of Farallon de Pajaros derived from GEBCO 2008 bathymetry. The contour colors correspond to the scale used in Figure 1a, with gray isolines indicating water depth at 500-m intervals. (c) Position of the H11S array 90-km south of Wake Island. The contour lines are spaced at 500-m intervals below sea level. (d) Tripartite configuration of the hydrophone elements at H11S.

and signs of gas emissions spotted at the sea surface southeast of Farallon de Pajaros (Global Volcanism Program, 2014). Over the course of the 15-day-long episode, broadband seismometers of the U.S. Geological Survey Northern Mariana Islands network (FDSN code MI) and hydrophones across the Pacific seaboard, located at distances of up to 12,000 km (cf. Tepp et al., 2017), registered a multitude of volcanoacoustic signals that were traced back to a location near Ahyi. The volcano was ultimately identified as the site of eruptive activity from repeat bathymetric mapping during a research expedition in May 2014, which showed that the summit area had given rise to a 100-m deep crater and shoaled by ~30 m compared to data collected in 2003 (Haney et al., 2014). Here the reader is referred to the Global Volcanism Program (2017) for a more comprehensive account of all follow-up investigations, since our study is primarily concerned with the hydroacoustic record of the 2014 episode.

Measuring long-range underwater sound can be an effective tool to overcome the observational limitations inherent to the study of submarine volcanism. In the global ocean, sound waves below a few hundred hertz travel in the Sound Fixing and Ranging channel (Ewing et al., 1951; Tolstoy et al., 1949), a distinct layer of minimum acoustic velocity that facilitates acoustic propagation over distances of hundreds to thousands of kilometers. For example, hydroacoustic phases associated with the 2011 eruption at Monowai, a volcanic center in the Kermadec Arc, were recorded over a source-receiver range of 15,800 km (Metz et al., 2016). Recent observations of submarine eruptions in the Mariana Arc region include long-range hydrophone recordings of explosive activity at Anatahan Volcano (Dziak et al., 2005), NW-Rota-1 (Chadwick et al., 2012; Schnur et al., 2017), and South Sarigan Seamount (Green et al., 2013).

The detection of underwater sound phases is one of the primary tasks of the International Monitoring System (IMS), a global sensor network put in place as part of the verification regime for the Comprehensive Nuclear-Test-Ban Treaty (CTBT). Six hydrophone stations, typically configured as triplet receiver arrays and moored in the deep sound channel, are in operation worldwide to detect nuclear explosions in the global ocean. However, IMS hydrophone data have implications beyond the realm of test-ban monitoring, for example, when studying tsunami signals (Matsumoto et al., 2016), and sources of low-frequency ocean noise (Woolfe & Sabra, 2015). Here we focus on recordings of IMS station H11 at Wake Island, where hydroacoustic arrivals associated with the 2014 eruption at Ahyi were recorded across the northwestern Pacific basin and over a geodesic distance of 2,283 km.

2. Hydrophone Triplet Data and Processing

2.1. Instrumentation

Station H11 of the IMS consists of two bottom moored hydrophone arrays, located approximately 55 km northeast (H11N) and 90 km south (H11S) of Wake Island (Figure 1b). The three hydrophones H11S1–3 are positioned on top of a 1,200-m deep seamount and moored near the local Sound Fixing and Ranging channel axis at approximately 740-m water depth (Figure S1 in the supporting information), with elements organized in a tripartite configuration and equidistant spacing of ~2 km (Figure 1c). Acoustic measurements are made at 250 Hz and transmitted in near-real time to the International Data Centre in Vienna for routine processing and analyst review (Hanson et al., 2001).

Peak acoustic amplitudes of hydroacoustic arrivals associated with volcanic activity at Ahyi are up to 5 dB higher at H11S than at H11N. The magnitude of the offset is consistent with observations by Heaney et al. (2013) for signals of the 2010 eruption at South Sarigan Seamount and most likely reflects different degrees of transmission loss due to bathymetric blockage and scattering along the source-receiver paths. We further note that background noise levels during times of acoustic quiescence are 1–2 dB lower at H11S, resulting in an overall higher signal-to-noise ratio compared to the northern array (factor 1.2 to 1.5). Therefore, our study focuses on the southern Wake Island hydrophone array.

2.2. Direction-of-Arrival Calculation and Detection

Hydrophone recordings are corrected for instrument response, and a mean and trend is removed. Data are band-pass filtered between 4 and 80 Hz to account for the broadband character of signals typically associated with submarine volcanic activity (Bohnenstiehl et al., 2014) and minimize potential noise contamination at both ends of the spectrum, for example, due to ocean microseism (Bromirski et al., 2005), marine mammal vocalization (Sousa & Harris, 2015), and commercial shipping (Sirovic et al., 2013). Since instruments are moored at similar water depths (740 ± 12 m) and the array aperture is multiple orders of magnitude smaller than the distance between Ahyi and H11S, direction-of-arrival calculations follow a two-dimensional plane wave fitting approach (Del Pezzo & Giudicepietro, 2002). Hydroacoustic recordings are subdivided into 1-min long, nonoverlapping windows (cf. Heaney et al., 2013; Metz et al., 2016). Peak delay times t_{ij} between instrument pairs located at relative positions x_{ij} are derived from normalized cross correlation of the windowed data. We obtain the slowness vector $p \equiv (p_x, p_y)$ of a planar wavefront moving across the triplet array by solving the following equation in a least square sense:

$$t_{ij} = p \cdot \Delta x_{ij} \tag{1}$$

Hence, apparent sound speed v and back azimuth θ are derived from

$$v = \left({p_x}^2 + {p_y}^2 \right)^{-1/2} \tag{2}$$

and

$$\theta = \tan^{-1}\left(p_x / p_y \right), \tag{3}$$

with errors of the least square solution obtained from the covariance matrix of the data according to Menke (2012).

To eliminate arrivals not traveling in the deep sound channel, 1-min windows with a sound speed below 1,400 or above 1,600 m/s are omitted from the data set (Hanson & Bowman, 2006). Derived travel time differences t_{ij}, t_{jk}, and t_{ki} between the three hydrophone pairs are summed to obtain the closure value cl of the windowed cross correlation. cl is assumed to approach zero for well-correlated signals and thus provides a quality constraint for extracting coherent acoustic phases from the ambient noise field (cf. Cansi, 1995):

$$cl = t_{ij} + t_{jk} + t_{ki} \tag{4}$$

The detection threshold of the closure function is set to a maximum of |48| ms, which corresponds to a mismatch of 12 sampling intervals at 250 Hz and is consistent with values used by Graeber and Piserchia (2004) for IMS hydrophone arrays in the Indian Ocean.

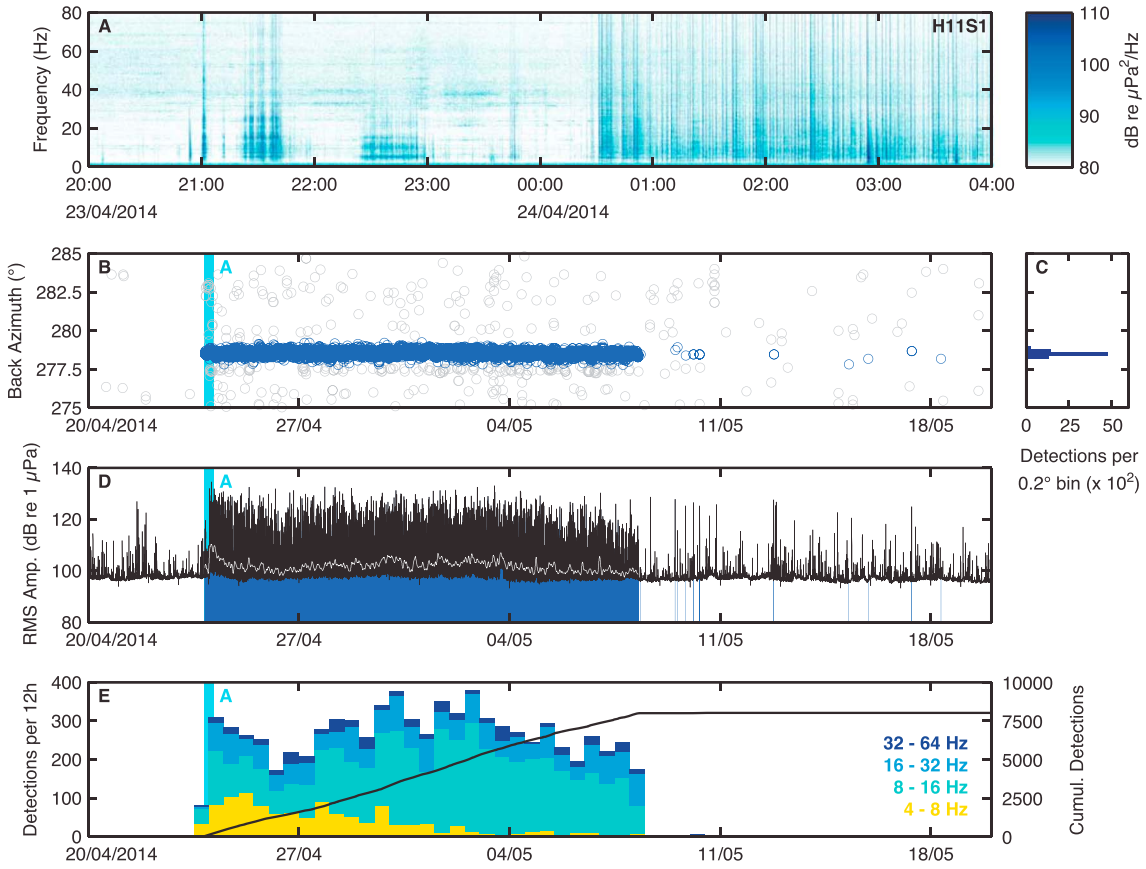

Figure 2. Hydroacoustic observations of volcanic activity at Ahyi. (a) Single receiver spectrogram of the H11S1 hydrophone data, beginning at 20:00:00 UTC 23 April 2014. A 1-Hz high-pass filter is applied to minimize background noise levels. (b) Back azimuths of 1-min detections between 20 April and 20 May 2014. (c) Arrivals associated with the eruption (blue circles) are symmetrically distributed around 278.5 ± 0.3° at two standard deviation uncertainty. (d) Root-mean-square amplitudes calculated over 1-min windows in the 4- to 80-Hz frequency band. For orientation, the white line indicates a 1-hr trend. The dark blue stems correspond to detections shown in Figure 2b and form a continuous band during the 15-day-long main burst of activity. (e) Detections from Ahyi per 12-hr interval and peak frequency distribution across four octave bands between 4 and 64 Hz. A cumulative sum of 8003 detections (black line) is registered between 21:00 UTC 23 April and 08:06 UTC 18 May 2014. The light blue area in the bottom three subplots marks the position of the 8-hr spectrogram shown in (a).

3. Hydroacoustic Observations

The 15-day-long main episode of volcanic activity at Ahyi begins at 00:30 UTC 24 April 2014, when the H11S hydrophone array registered high incidences of short (<15 s) transient arrivals spaced seconds to minutes apart and with sharp onset and termination, most likely representing an ensemble record of shallow volcano-tectonic seismicity and explosions in the frequency band of up to 80 Hz (Figure 2a). This main episode is preceded by a sequence of acoustic precursory events over the course of 3.5 hr: A minute-long, broadband impulse at 21:00 UTC 23 April, followed by two circa 30-min long bursts at 21:20 and 22:20 UTC. While the shape of the first signal strongly resembles a T phase generated by a shallow focus (<10 km) seismic event and is different from the elongated, low-frequency (<10 Hz) arrivals generated by tectonic earthquakes (Sugioka et al., 2000; Yang & Forsyth, 2003), the two bursts exhibit sustained peak frequencies at 16 (21:20 UTC) and 6 Hz (22:20 UTC) and thus could be interpreted as tremor caused by resonance in a fluid-filled crack or conduit (Chouet, 1996). We speculate that these precursory signals represent the initial breaching of the magma chamber walls and subsequent flow and pressure oscillations (Bohnenstiehl et al., 2013), which are then followed by the rise and opening of the magma-filled conduit and the onset of persistent activity during the main episode. In an alternative scenario, the spectral banding could be explained by the interference of seafloor and sea surface reflected acoustic phases that arrive at the H11S array with small time delays ("multipathing," cf. Dziak et al., 2015; Matsumoto et al., 2011). We note, however, that, since comparable arrivals are not observed during

later stages, this assumption fails to explain the distinct occurrence of harmonic signals at the beginning of the volcanic episode as well as the notably different fundamental frequencies of the two presumed tremor events.

Between 23 April and 8 May 2014, 1-min detections distinctly stabilize at a back azimuth of 278.5 ± 0.3° and within 0.5° of the geodesic angle of arrival for a source Ahyi (Figures 2b–2c). Although not used as a detection criterion, interhydrophone correlation coefficients of these 8,003 1-min windows on average exceed 0.4, with peak levels of up to 0.9, thus distinctly setting apart activity at the volcano from uncorrelated background noise (see also Figure S2). A small number of arrivals registered from ~277.6° at the time of the episode probably represent reflections off Maug Island. Notably, no activity at Ahyi is detected at H11S in the weeks prior to the 2014 event. Since our observations are in agreement with local eyewitness reports (cf. Global Volcanism Program, 2014) and seafloor topography suggests no other volcanically active sites along the great circle path between the volcano and the hydrophone array, we interpret low-frequency arrivals shown in Figures 2b and 2c (blue circles) to be associated with the eruption at Ahyi. During the 15-day-long main episode, RMS amplitudes exceed preeruption background levels by 10–30 dB and typically range from 100 to 130 dB re 1 μPa in the 4- to 80-Hz frequency band, with 180 to 380 1-min detections counted per 12-hr interval (Figures 2d and 2e). An initial ramp up and drop in acoustic activity over the first 3 days of the main episode is followed by a period of gradual increase and decline of RMS levels and detection rate over approximately 12 consecutive days. We interpret the first part of this progression as an initial phase of stress release, possibly involving the formation of the newly developed, 95-m-deep summit crater due to the ejection of material near the top of the volcano (cf. Watts et al., 2012) or in response to the deflation of a shallow magma reservoir (e.g., Fornari et al., 1984). This initial phase then is succeeded by a prolonged stage of repressurization until the system regains equilibrium and the volcano becomes acoustically dormant again. After 8 May, only a dozen isolated, explosion-type arrivals are registered by the H11 hydrophones.

In a further step, we assess the peak frequency distribution of the 1-min detections in four octave bands between 4 and 64 Hz over the course of the eruption (Figure 2e). While arrivals in the upper bands follow a relatively uniform distribution over time, there is a notable decline in detections with peak frequencies below 8 Hz that become near absent during the second half of the episode. This trend can be observed at both H11 hydrophone arrays and is not found in the data of 1-min windows eliminated during processing, that is, the ambient ocean noise field. Hence, we interpret the decrease in low-frequency arrivals as a change in signal source parameters. Since volcanoacoustic signals at frequencies below ~10 Hz are typically associated with fluid movement and oscillation in highly pressurized systems (e.g., Matoza & Chouet, 2010; Neuberg et al., 2006), their gradual cessation may be due to lower pressure gradients and subsequently reduced magma flow within, or into, the volcanic conduit toward the end of the eruption. In contrast, higher frequency events typically result from brittle fracture and, in a submarine environment, explosions at the seafloor-ocean interface (cf. Caplan-Auerbach et al., 2017), which would explain their continuous presence throughout the episode.

4. Resolution and Seismic Magnitude Estimate

Root-mean-square levels of the 8,003 1-min detections associated with volcanic activity at Ahyi follow a right-skewed normal distribution with a steep decline toward lower amplitudes (Figure 3a), indicating that events below a certain threshold may not be fully detected. We therefore derive the acoustic resolution of the data set according to the maximum curvature method by Wiemer and Katsumata (1999), in which the data bin with the highest number of detections represents the sound pressure level above that all arrivals can be successfully identified. In the case of volcanic activity at Ahyi, acoustic resolution is assumed to be 98 dB re 1 μPa.

In order to infer comparable seismic magnitudes of events at Ahyi, we relate acoustic and seismic measurements of tectonic earthquakes registered by the global IMS network along the central Mariana Arc (Figure 3b). We account for potential attenuation of the earthquake signal in the solid Earth and along the deep sound channel by limiting the data set to events with a catalogued depth of less than 80 km and a source-receiver distance similar to the great circle path between Ahyi and the southern Wake Island array, that is, 2,283 ± 250 km. Since RMS amplitudes are routinely calculated over the entire length of the arrival

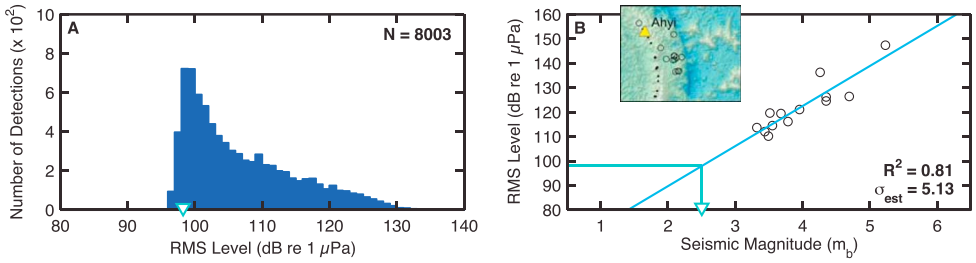

Figure 3. Resolution and comparable seismic magnitude. (a) Root-mean-square (RMS) amplitude distribution of 1-min detections recorded at International Monitoring System (IMS) hydrophone H11S1. Data are binned to 1-dB intervals. The green triangle marks the level of acoustic resolution at 98-dB re 1 μPa, calculated according to Wiemer and Katsumata (1999). (b) RMS pressure amplitude of 13 earthquakes (black circles) registered by the IMS seismic network and hydrophone H11S1 between 2012 and 2017. Events are located along the central Mariana arc at 2,283 ± 250-km distance from the H11S array and up to 80-km focal depth (see inset for epicenter locations). Body wave magnitudes are given at an absolute uncertainty of 0.1 m_b or less. The linear relationship between acoustic and seismic magnitude (bright blue line) is significant at $R^2 = 0.81$ and an error of 5.13 dB. Following the derived trend, acoustic resolution of 98 dB re 1 μPa corresponds to a body wave magnitude of 2.5 m_b (green line and triangle).

in the IMS processing stream, data are further constrained to events with an arrival length of 40 to 80 s at the H11S1 hydrophone to match the 1-min segmentation of our aggregate approach. The equation of the regression line in Figure 3b

$$\text{RMS Level (dB re 1 μPa)} = 56.9 + 16.3m_b \tag{5}$$

indicates a linear relationship between acoustic and seismic magnitude (R^2 = 0.81) and is consistent with observations by Pulli and Upton (2002) for earthquakes in the Indian Ocean. A minimum seismic magnitude of 2.5 m_b, corresponding to the acoustic resolution of 98 dB, can be successfully resolved at H11S1 and is almost one order lower than the smallest tectonic earthquake detected by the global IMS seismometer network in the central Mariana Trench region. Using the derived trend as a first-order approximation, we estimate comparable body wave magnitudes for events at Ahyi between 2.5 and 4.6 m_b, which is, for example, similar to presumed levels of activity at Brothers Volcano (2.4 to 3.2 m_b) in the Kermadec Arc (Dziak et al., 2008), and at Fukutoku-Okanoba in the Volcano Islands (3.5 to 4.7 m_b, Dziak & Fox, 2002). We note that some bias may be introduced due to data segmentation, as more than one transient signal from Ahyi can be present in a given 1-min window. Hence, our approach may overestimate acoustic RMS amplitudes and, subsequently, inferred levels of seismicity. It is therefore possible that the acoustic resolution of the hydrophone array for events at the volcano may be even lower than presented here.

5. Acoustic Energy Release

Due to its potentially harmful effect on marine ecosystems, underwater noise from anthropogenic sources, in particular commercial shipping (McKenna et al., 2012) and seismic exploration (Nieukirk et al., 2004), has become an increasingly relevant topic in ocean conservation and policy making (e.g., Papanicolopulu, 2011; Williams et al., 2015). Yet there exists little knowledge on the contribution of solid Earth processes, that is, earthquakes and volcanic activity, to the ocean soundscape. Following procedures outlined by Hildebrand (2009) and previously implemented by Bohnenstiehl et al. (2013), we therefore attempt to quantify the amount of acoustic energy radiated into the water column during the 2014 eruption at Ahyi.

In a first step, acoustic intensity I of a source in the far field is derived from (units in brackets)

$$I = \frac{p^2}{z} \quad \left(W/\text{m}^2\right) \tag{6}$$

where p represents the source pressure level at 1-m distance and the specific acoustic impedance z is given as the product of the nominal density and sound speed of seawater, fixed at 1,030 kg/m^3 and 1,480 m/s,

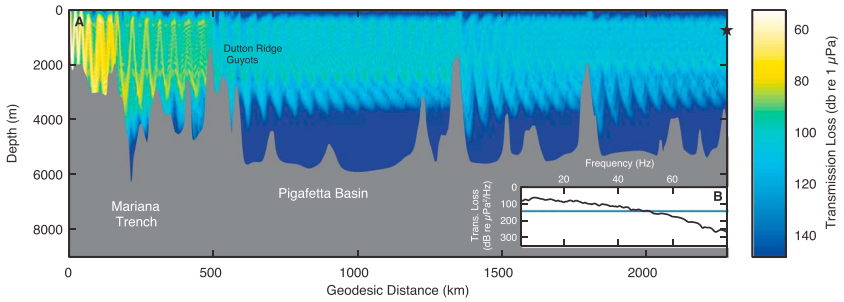

Figure 4. Transmission loss estimates obtained from a two-dimensional parabolic equation model (RAM, Collins, 1993). (a) Exemplary source-receiver profile for a 32-Hz signal between Ahyi and the H11S1 hydrophone (black line in Figure 1a). The instrument is moored at a distance of 2,283 km and near 750-m water depth (black star). The model assumes a source at 70 m below sea level, corresponding to the approximate summit depth of the volcano. Bottom properties are set to 1,700 and 2,200 m/s for sound speed, with corresponding attenuation parameters of 0.3 above and 0.05 dB/m/kHz up to 150 m below the seafloor, respectively. Sound speed profiles are calculated every kilometer according to Mackenzie (1981), using water column data provided by the 2005 World Ocean Atlas. Bathymetry is taken from the 2008 GEBCO grid and sampled at 100-m intervals. (b) Transmission loss for frequencies in the 4- to 80-Hz band (black line) calculated at 0.2-Hz intervals and smoothed using a 1-Hz-wide moving-average filter. The blue line marks the mean at 141 dB re 1 μPa at 1 m.

respectively. Assuming that energy at the volcano is released into an acoustic half-space, we calculate the signal power P as the product of intensity and the geometric factor 2π (m^2):

$$P = I \times 2\pi \quad (J/s) \tag{7}$$

Finally, acoustic energy E is defined as the integral of the intensity over source region and time. Here it is expressed as the linear product of power and duration (T):

$$E = P \times T \quad (J) \tag{8}$$

The above calculations are carried out in nonoverlapping windows of the length T = 1 s within the 8,003 1-min detections registered at hydrophone H11S1 between 23 April and 8 May 2014, resulting in a total of 480,180 measurements that are summed to obtain the total energy released during the eruption. Background noise levels of 97 dB, corresponding to 1 dB below the acoustic resolution of the array, are removed beforehand (Holt et al., 2009). Results from two-dimensional, range-dependent parabolic equation modeling (Collins, 1993) indicate a mean transmission loss of 141 dB along the 2,283–km-long source-receiver path for signals in the 4- to 80-Hz band (Figure 4) and are accounted for in the subsequent calculation of pressure levels referenced to 1-m distance from the source (Matsumoto et al., 2011).

Results show that during the eruptive episode, source levels at Ahyi were on the order of 245–275 dB re 1 μPa at 1 m and a total of 9.7 10^{13} J of acoustic energy was radiated in the 4- to 80-Hz band over the course of 8,003 min (~5.6 days). The yield estimate is similar to calculations by Bohnenstiehl et al. (2013), who use a set of regional hydrophone stations (140- to 400-km source-receiver distance) to investigate the 2009 eruption at Hunga Ha'apai-Hunga Tonga volcano in the Tonga Arc (1.7 to 4.7 10^{13} J over 2.7 days). This confirms that the contribution of submarine volcanic activity at Ahyi to the ocean soundscape is indeed substantial. For example, acoustic energy released at the volcano supersedes the projected annual input from seismic surveying by a factor of two (3.9 10^{13} J, Hildebrand, 2005) and is almost four times higher than previous estimates for the cumulative energy of all sonar activities in the global ocean combined (2.6 10^{13} J, Hildebrand, 2005). However, unlike underwater noise produced by sonar, ship traffic and seismic surveying, volcanic episodes represent intense, yet localized and often short-lived events. Hence, their ecological impact remains difficult to assess, and it is not known to which degree marine mammals are affected by, or have become habituated to, these natural sources of low-frequency sound.

6. Conclusion

An IMS hydrophone station located at Wake Island, Northwest Pacific Ocean, detected underwater sound phases associated with the 2014 eruption at Ahyi. Volcanic activity occurred in two bursts over the course of 15 days, preceded only by a 3.5-hr-long period of precursory events. There is a notable absence in low-frequency (<8 Hz) arrivals during the later stages of the eruption, which could be interpreted as the result of decreasing pressure gradients and subsequent reduction in fluid movement in the volcanic system. We exploit the linear relationship between acoustic RMS amplitude and body wave magnitude of shallow tectonic earthquakes along the Mariana Arc to approximate the seismic range of activity at Ahyi. The resolution of the H11S hydrophone array supersedes broadband network data by more than half a magnitude and places seismic events at Ahyi between 2.5 and 4.6 m_b. Acoustic energy released during the eruption is on the order of 9.7 10^{13} J, suggesting that the contribution of solid Earth sources to the ocean soundscape may be much higher than previously thought. Our findings highlight the potential of the Wake Island hydrophone array for remotely studying volcanic activity at Ahyi and may aid in detecting further active sites along the Mariana Arc, and elsewhere, in the future.

Disclaimer

The views expressed in this study are those of the authors and do not necessarily reflect those of the Preparatory Commission for the CTBTO.

Acknowledgments

Hydroacoustic data were made available by the CTBTO International Data Centre, Vienna, through the virtual Data Exploitation Centre (vDEC, www.ctbto.org/specials/vdec/), and processed using MATLAB-based tools, including GISMO (https://geoscience-community-codes.github.io/GISMO/) and the Waveform Suite (Reyes & West, 2011). Albert Brouwer (CTBTO) advised on IMS instrumentation and database access. The authors thank Ronan Le Bras (CTBTO) and Läslo Evers (KNMI) for their insightful comments on an early version of the manuscript. Reviews provided by the editor Rebecca Carey, Jelle Assink, and an anonymous reviewer further improved this article.

References

Bloomer, S. H., Stern, R. J., & Smoot, N. C. (1989). Physical volcanology of the submarine Mariana and volcano arcs. *Bulletin of Volcanology*, *51*(3), 210–224. https://doi.org/10.1007/BF01067957

Bohnenstiehl, D. R., Dziak, R. P., Matsumoto, H., & Conder, J. A. (2014). Acoustic response of submarine volcanoes in the Tofua Arc and northern Lau Basin to two great earthquakes. *Geophysical Journal International*, *196*(3), 1657–1675. https://doi.org/10.1093/gji/ggt472

Bohnenstiehl, D. R., Dziak, R. P., Matsumoto, H., & Lau, T. K. A. (2013). Underwater acoustic records from the March 2009 eruption of Hunga Ha'apai-Hunga Tonga volcano in the Kingdom of Tonga. *Journal of Volcanology and Geothermal Research*, *249*, 12–24. https://doi.org/10.1016/j.jvolgeores.2012.08.014

Bromirski, P. D., Duennebier, F. K., & Stephen, R. A. (2005). Mid-ocean microseisms. *Geochemistry, Geophysics, Geosystems*, *6*, Q04009. https://doi.org/10.1029/2004GC000768

Cansi, Y. (1995). An automatic seismic event processing for detection and location: The P.M.C.C. method. *Geophysical Research Letters*, *22*, 1021–1024. https://doi.org/10.1029/95GL00468

Caplan-Auerbach, J., Dziak, R. P., Haxel, J., Bohnenstiehl, D. R., & Garcia, C. (2017). Explosive processes during the 2015 eruption of Axial Seamount, as recorded by seafloor hydrophones. *Geochemistry, Geophysics, Geosystems*, *18*, 1761–1774. https://doi.org/10.1002/2016GC006734

Chadwick, W. W. J., Dziak, R. P., Haxel, J. H., Embley, R. W., & Matsumoto, H. (2012). Submarine landslide triggered by volcanic eruption recorded by in situ hydrophone. *Geology*, *40*(1), 51–54. https://doi.org/10.1130/G32495.1

Chouet, B. A. (1996). Long-period volcano seismicity: Its source and use in eruption forecasting. *Nature*, *380*(6572), 309–316. https://doi.org/10.1038/380309a0

Collins, M. D. (1993). A split-step pade solution for the parabolic equation method. *The Journal of the Acoustical Society of America*, *93*(4), 1736–1742. https://doi.org/10.1121/1.406739

Del Pezzo, E., & Giudicepietro, F. (2002). Plane wave fitting method for a plane, small aperture, short period seismic array: A MATHCAD program. *Computational Geosciences*, *28*(1), 59–64. https://doi.org/10.1016/S0098-3004(01)00076-0

Dziak, R. P., Bohnenstiehl, D. R., Baker, E. T., Matsumoto, H., Caplan-Auerbach, J., Embley, R. W., et al. (2015). Long-term explosive degassing and debris flow activity at West Mata submarine volcano. *Geophysical Research Letters*, *42*, 1480–1487. https://doi.org/10.1002/2014GL062603

Dziak, R. P., & Fox, C. G. (2002). Evidence of harmonic tremor from a submarine volcano detected across the Pacific Ocean basin. *Journal of Geophysical Research*, *107*(B5), 2085. https://doi.org/10.1029/2001JB000177

Dziak, R. P., Haxel, J. H., Matsumoto, H., Lau, T. K. A., Merle, S. G., de Ronde, C. E. J., et al. (2008). Observations of regional seismicity and local harmonic tremor at Brothers volcano, south Kermadec arc, using an ocean bottom hydrophone array. *Journal of Geophysical Research*, *113*, B08S04. https://doi.org/10.1029/2007JB005533

Dziak, R. P., Park, M., Matsumoto, H., & Byun, S. K. (2005). Hydroacoustic records and a numerical model of the source mechanism from the first historical eruption of Anatahan volcano, Mariana Islands. *Journal of Volcanology and Geothermal Research*, *146*(1–3), 86–101. https://doi.org/10.1016/j.jvolgeores.2004.12.009

Ewing, M., Press, F., & Worzel, J. L. (1951). Further observations of the T-phase. *Geological Society of America Bulletin*, *62*(12), 1527–1527.

Fornari, D. J., Ryan, W. B. F., & Fox, P. J. (1984). The evolution of craters and calderas on young seamounts: Insights from SEA MARC I and SEA beam sonar surveys of a small seamount group near the axis of the East Pacific Rise at ~10°N. *Journal of Geophysical Research*, *89*, 11,069–11,083. https://doi.org/10.1029/JB089iB13p11069

Global Volcanism Program (1979). Report on Ahyi (United States), edited by D. Squires. *Scientific Event Alert Network Bulletin*, *4*(11). https://doi.org/10.5479/si. GVP.SEAN197911-284141

Global Volcanism Program (2001). Report on Ahyi (United States), edited by R. Wunderman. *Bulletin of the Global Volcanism Network*, *26*(5). https://doi.org/10.5479/si. GVP.BGVN200105-284141

Global Volcanism Program (2013). Volcanoes of the world, Smithsonian Institution, Edited by E. Venzke. https://doi.org/10.5479/si.GVP.VOTW4-2013

Global Volcanism Program (2014). Report on Ahyi (United States), edited by R. Wunderman. *Bulletin of the Global Volcanism Network*, *39*(2). https://doi.org/10.5479/si. GVP.BGVN201402-284141

Global Volcanism Program (2017). Report on Ahyi (United States), edited by E. Venzke.

Graeber, F. M., & Piserchia, P.-F. (2004). Zones of T-wave excitation in the NE Indian ocean mapped using variations in backazimuth over time obtained from multi-channel correlation of IMS hydrophone triplet data. *Geophysical Journal International*, *158*(1), 239–256. https://doi.org/10.1111/j.1365-246X.2004.02301.x

Green, D. N., Evers, L. G., Fee, D., Matoza, R. S., Snellen, M., Smets, P., & Simons, D. (2013). Hydroacoustic, infrasonic and seismic monitoring of the submarine eruptive activity and sub-aerial plume generation at South Sarigan, May 2010. *Journal of Volcanology and Geothermal Research*, *257*, 31–43. https://doi.org/10.1016/j.jvolgeores.2013.03.006

Haney, M. M., Chadwick, W., Merle, S. G., Buck, N. J., Butterfield, D. A., Coombs, M. L., et al. (2014). The 2014 submarine eruption of Ahyi volcano, Northern Mariana Arc.

Hanson, J., Le Bras, R., Dysart, P., Brumbaugh, D., Gault, A., & Guern, J. (2001). Operational processing of hydroacoustics at the Prototype International Data Center. *Pure and Applied Geophysics*, *158*(3), 425–456. https://doi.org/10.1007/PL00001190

Hanson, J. A., & Bowman, J. R. (2006). Methods for monitoring hydroacoustic events using direct and reflected T waves in the Indian Ocean. *Journal of Geophysical Research*, *111*, B02305. https://doi.org/10.1029/2004JB003609

Heaney, K. D., Campbell, R. L., & Snellen, M. (2013). Long range acoustic measurements of an undersea volcano. *The Journal of the Acoustical Society of America*, *134*(4), 3299–3306. https://doi.org/10.1121/1.4818844

Hildebrand, J. A. (2005). Impacts of anthropogenic sound. In J. E. Reynolds, III, W. F. Perrin, R. R. Reeves, S. Montgomery, & T. J. Ragen (Eds.), *Marine Mammal Research Conservation beyond Crisis* (pp. 101–124). Baltimore: Johns Hopkins University Press.

Hildebrand, J. A. (2009). Anthropogenic and natural sources of ambient noise in the ocean. *Marine Ecology Progress Series*, *395*, 5–20. https://doi.org/10.3354/meps08353

Holt, M. M., Noren, D. P., Veirs, V., Emmons, C. K., & Veirs, S. (2009). Speaking up: Killer whales (Orcinus orca) increase their call amplitude in response to vessel noise. *The Journal of the Acoustical Society of America*, *125*(1), EL27–EL32. https://doi.org/10.1121/1.3040028

Mackenzie, K. V. (1981). 9-term equation for sound speed in the oceans. *The Journal of the Acoustical Society of America*, *70*(3), 807–812. https://doi.org/10.1121/1.386920

Matoza, R. S., & Chouet, B. A. (2010). Subevents of long-period seismicity: Implications for hydrothermal dynamics during the 2004–2008 eruption of Mount St. Helens. *Journal of Geophysical Research*, *115*, B12206. https://doi.org/10.1029/2010JB007839

Matsumoto, H., Haralabus, G., Zampolli, M., & Oezel, N. M. (2016). T-phase and tsunami pressure waveforms recorded by near-source IMS water-column hydrophone triplets during the 2015 Chile earthquake. *Geophysical Research Letters*, *43*, 12,511–12,519. https://doi.org/10.1002/2016GL071425

Matsumoto, H., Haxel, J. H., Dziak, R. P., Bohnenstiehl, D. R., & Embley, R. W. (2011). Mapping the sound field of an erupting submarine volcano using an acoustic glider. *The Journal of the Acoustical Society of America*, *129*(3), EL94–EL99. https://doi.org/10.1121/1.3547720

McKenna, M. F., Katz, S. L., Wiggins, S. M., Ross, D., & Hildebrand, J. A. (2012). A quieting ocean: Unintended consequence of a fluctuating economy. *The Journal of the Acoustical Society of America*, *132*(3), EL,169–EL,175. https://doi.org/10.1121/1.4740225

Menke, W. (2012). Chapter 4—Solution of the linear, Gaussian inverse problem, viewpoint 2: General inverses. In W. Menke (Ed.), *Geophysical Data Analysis: Discrete Inverse Theory* (3rd ed., pp. 69–88). Waltham, MA: American Press. https://doi.org/10.1016/B978-0-12-397160-9.00,004-7

Metz, D., Watts, A. B., Grevemeyer, I., Rodgers, M., & Paulatto, M. (2016). Ultra-long-range hydroacoustic observations of submarine volcanic activity at Monowai, Kermadec Arc. *Geophysical Research Letters*, *43*, 1529–1536. https://doi.org/10.1002/2015GL067259

Neuberg, J. W., Tuffen, H., Collier, L., Green, D., Powell, T., & Dingwell, D. (2006). The trigger mechanism of low-frequency earthquakes on Montserrat. *Journal of Volcanology and Geothermal Research*, *153*(1–2), 37–50. https://doi.org/10.1016/j.jvolgeores.2005.08.008

Nieukirk, S. L., Stafford, K. M., Mellinger, D. K., Dziak, R. P., & Fox, C. G. (2004). Low-frequency whale and seismic airgun sounds recorded in the mid-Atlantic Ocean. *The Journal of the Acoustical Society of America*, *115*(4), 1832–1843. https://doi.org/10.1121/1.1675816

Norris, R. A., & Johnson, R. H. (1969). Submarine volcanic eruptions recently located in the Pacific by Sofar hydrophones. *Journal of Geophysical Research*, *74*, 650–664. https://doi.org/10.1029/JB074i002p00650

Papanicolopulu, I. (2011). The European Union and the regulation of underwater noise pollution. In D. Vidas & P. J. Schei (Eds.), *The World Ocean in Globalisation* (pp. 457–471). Leiden, Netherlands: Martinus Nijhoff Publishers. https://doi.org/10.1163/9789004204225_025

Pulli, J. J., & Upton, Z. M. (2002). Hydroacoustic observations of Indian earthquake provide new data on T-waves. *Eos*, *83*(13), 145–151. https://doi.org/10.1029/2002EO000090

Resing, J. A., Baker, E. T., Lupton, J. E., Walker, S. L., Butterfield, D. A., Massoth, G. J., & Nakamura, K.-I. (2009). Chemistry of hydrothermal plumes above submarine volcanoes of the Mariana Arc. *Geochemistry, Geophysics, Geosystems*, *10*, Q02009. https://doi.org/10.1029/2008GC002141

Reyes, C. G., & West, M. E. (2011). The waveform suite: A robust platform for manipulating waveforms in MATLAB. *Seismological Research Letters*, *82*(1), 104–110. https://doi.org/10.1785/gssrl.82.1.104

Schnur, S. R., Chadwick, W. W. Jr., Embley, R. W., Ferrini, V. L., de Ronde, C. E. J., Cashman, K. V., et al. (2017). A decade of volcanic construction and destruction at the summit of NW Rota-1 seamount: 2004–2014. *Journal of Geophysical Research: Solid Earth*, *122*, 1558–1584. https://doi.org/10.1002/2016JB013742

Sirovic, A., Wiggins, S. M., & Oleson, E. M. (2013). Ocean noise in the tropical and subtropical Pacific Ocean. *The Journal of the Acoustical Society of America*, *134*(4), 2681–2689. https://doi.org/10.1121/1.4820884

Sousa, A. G., & Harris, D. (2015). Description and seasonal detection of two potential whale calls recorded in the Indian Ocean. *The Journal of the Acoustical Society of America*, *138*(3), 1379–1388. https://doi.org/10.1121/1.4928719

Sugioka, H., Fukao, Y., Kanazawa, T., & Kanjo, K. (2000). Volcanic events associated with an enigmatic submarine earthquake. *Geophysical Journal International*, *142*(2), 361–370. https://doi.org/10.1046/j.1365-246x.2000.00153.x

Tepp, G., Haney, M., Lyons, J., Dziak, R., Haxel, J., Bohnenstiehl, D., & Chadwick, W. (2017). The sounds of submarine volcanoes. *The Journal of the Acoustical Society of America*, *142*(4), 2486–2486. https://doi.org/10.1121/1.5014073

Tolstoy, I., Ewing, M., & Press, F. (1949). T phase of shallow-focus submarine earthquakes. *Geological Society of America Bulletin*, *60*(12), 1957–1957.

Watts, A. B., Peirce, C., Grevemeyer, I., Paulatto, M., Stratford, W., Bassett, D., et al. (2012). Rapid rates of growth and collapse of Monowai volcano in the Karmadec Arc. *Nature Geoscience*, *5*(7), 510–515. https://doi.org/10.1038/ngeo1473

Wiemer, S., & Katsumata, K. (1999). Spatial variability of seismicity in aftershock zones. *Journal of Geophysical Research*, *104*, 13,135–13,151. https://doi.org/10.1029/1999JB900032

Williams, R., Wright, A. J., Ashe, E., Blight, L. K., Bruintjes, R., Canessa, R., et al. (2015). Impacts of anthropogenic noise on marine life: Publication patterns, new discoveries, and future directions in research and management. *Ocean and Coastal Management*, *115*(C), 17–24. https://doi.org/10.1016/j.ocecoaman.2015.05.021

Woolfe, K. F., & Sabra, K. G. (2015). Variability of the coherent arrivals extracted from low-frequency deep-ocean ambient noise correlations. *The Journal of the Acoustical Society of America*, *138*(2), 521–532. https://doi.org/10.1121/1.4923447

Yang, Y. J., & Forsyth, D. W. (2003). Improving epicentral and magnitude estimation of earthquakes from T phases by considering the excitation function. *Bulletin of the Seismological Society of America*, *93*(5), 2106–2122. https://doi.org/10.1785/0120020215